



*Supplement of*

## **Relationship between latent and radiative heating fields of tropical cloud systems using synergistic satellite observations**

**Xiaoting Chen et al.**

*Correspondence to:* Xiaoting Chen ([xiaoting.chen@lmd.ipsl.fr](mailto:xiaoting.chen@lmd.ipsl.fr))

The copyright of individual parts of the supplement might differ from the article licence.

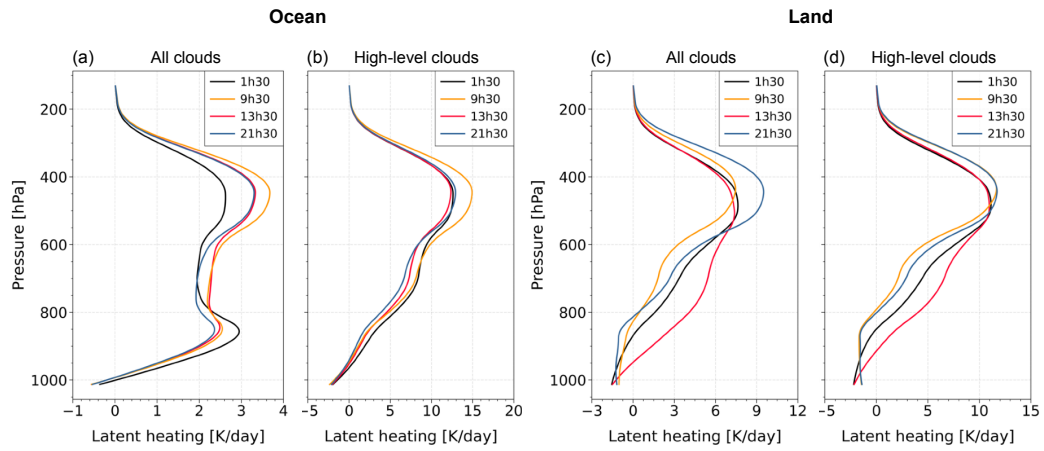


**Figure S1.** TRMM-SLH LH profiles of precipitating cloud scenes (a,c) and precipitating high-level clouds (b,d) at 4 observation times (1h30, 9h30 AM/PM), separately over ocean (a,b) and over land (c,d), Data are averaged over the TRMM-CIRS collocated data during the period 2008–2013, within  $30^{\circ}\text{N}$ – $30^{\circ}\text{S}$ , with a spatial resolution of  $0.5^{\circ}$ .

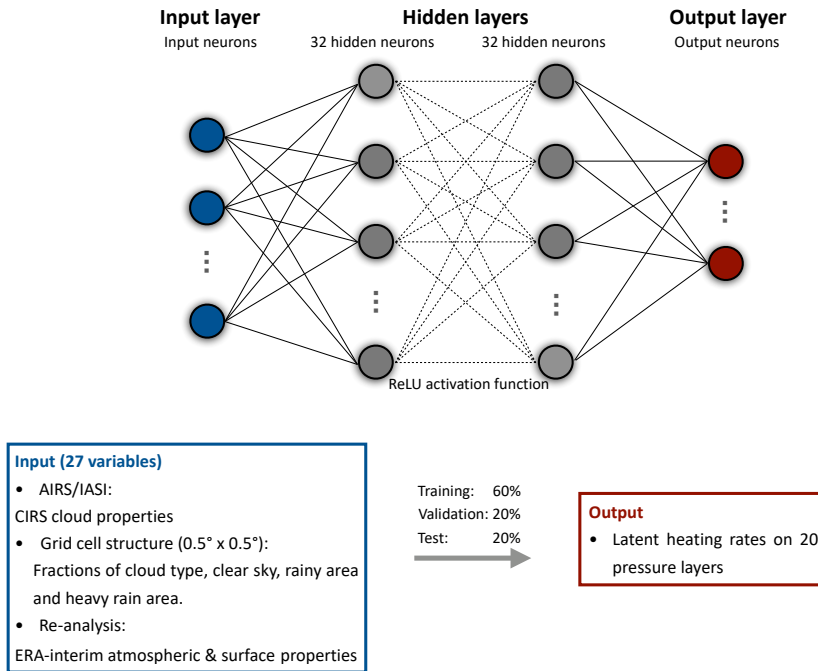


**Figure S2.** Structure of the ANN used in this study for latent heating retrieval. The network takes 27 input variables and processes them through two hidden layers to predict a latent heating profile within 20 pressure layers as the output. Blue nodes represent input neurons, gray nodes represent hidden neurons, and red nodes indicate the final output neurons.

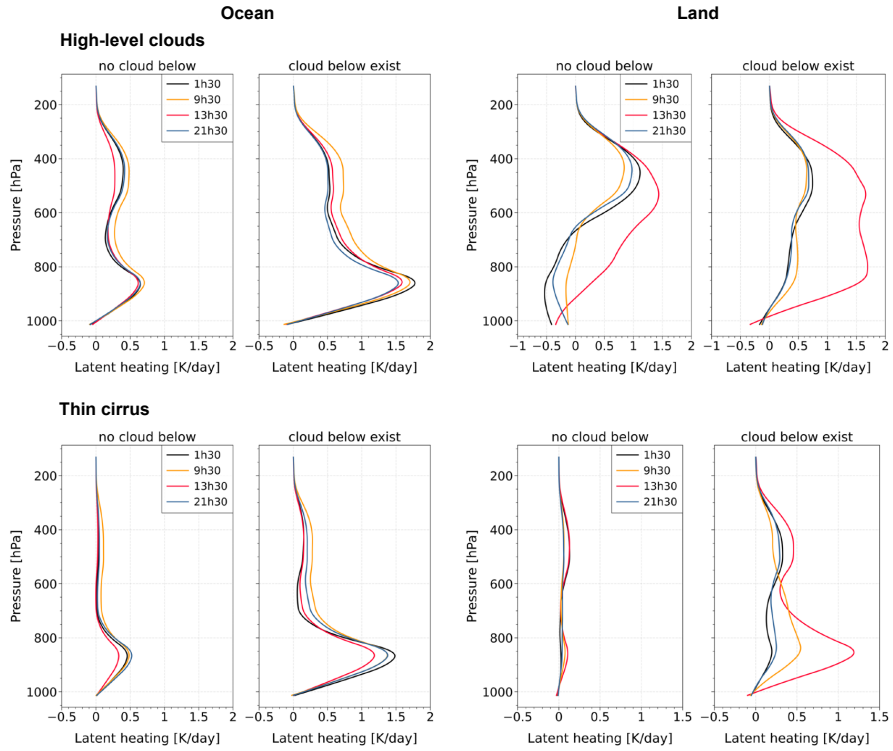


**Figure S3.** TRMM-SLH LH profiles of non-precipitating high-level clouds (top panels) and thin Cirrus (bottom panels) at 4 observation times (1h30, 9h30 AM/PM), considering the absence or presence of underlying lower clouds (no cloud below, cloud below exist) from CIRS-ML, separately over ocean (left) and over land (right). Data are averaged over the TRMM-CIRS collocated data during the period 2008–2013, within 30°N–30°S, at a spatial resolution of 0.5°.

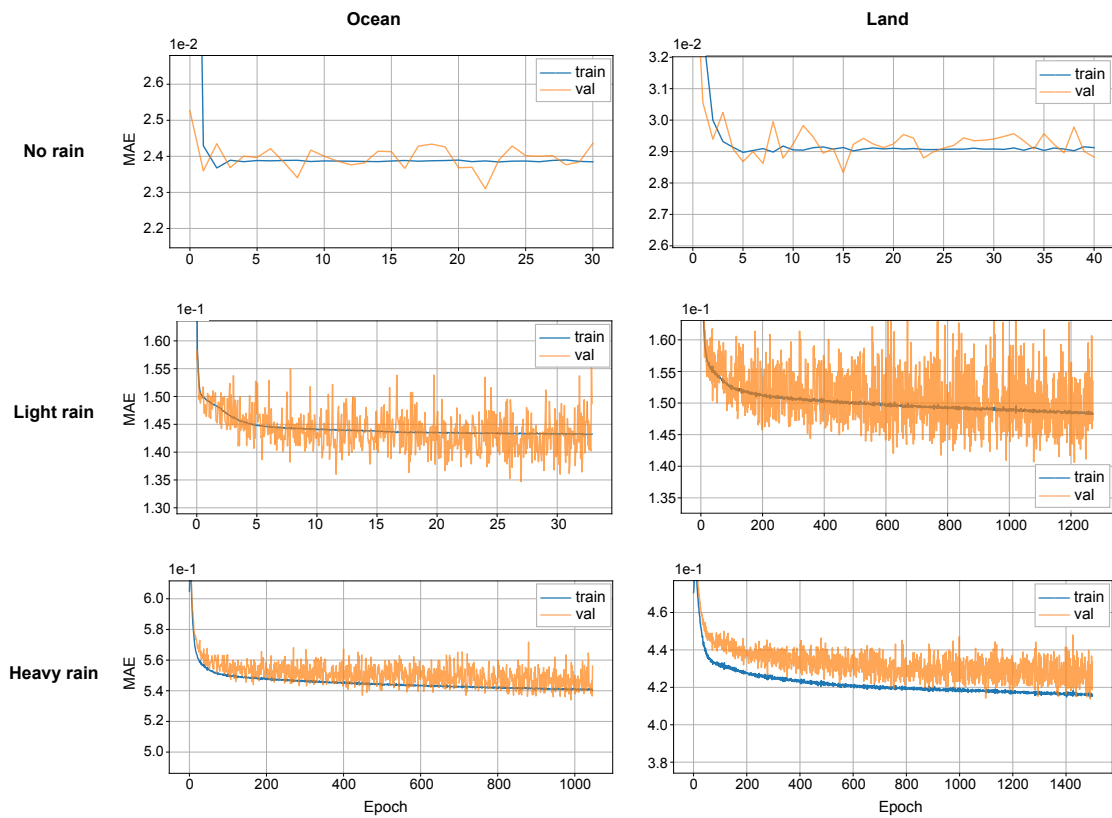


**Figure S4.** Mean absolute error (MAE) as a function of iterations (epochs) for high-level clouds, categorized by three rain intensities (top to bottom: no rain, light rain, heavy rain) over ocean (left) and land (right). ANN regressions were trained on collocated AIRS–TRMM data.

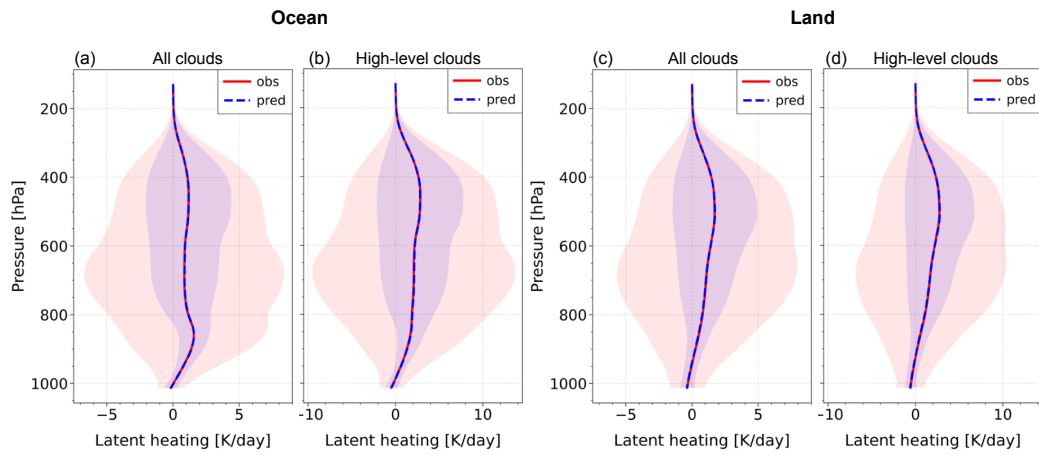


**Figure S5.** Average and range of predicted (dashed) and observed (solid) latent heating (2004–2013) for (a,c) all cloud scenes and (b,d) high-level clouds 1h30 AM/PM (AIRS), separately over ocean (a,b) and over land (c,d), within  $30^{\circ}\text{N}$ – $30^{\circ}\text{S}$ , with a spatial resolution of  $0.5^{\circ}$ . Models were trained on collocated AIRS–TRMM. Shaded areas indicate  $\pm 67.5\%$  of the standard deviation, which corresponds to quartiles.

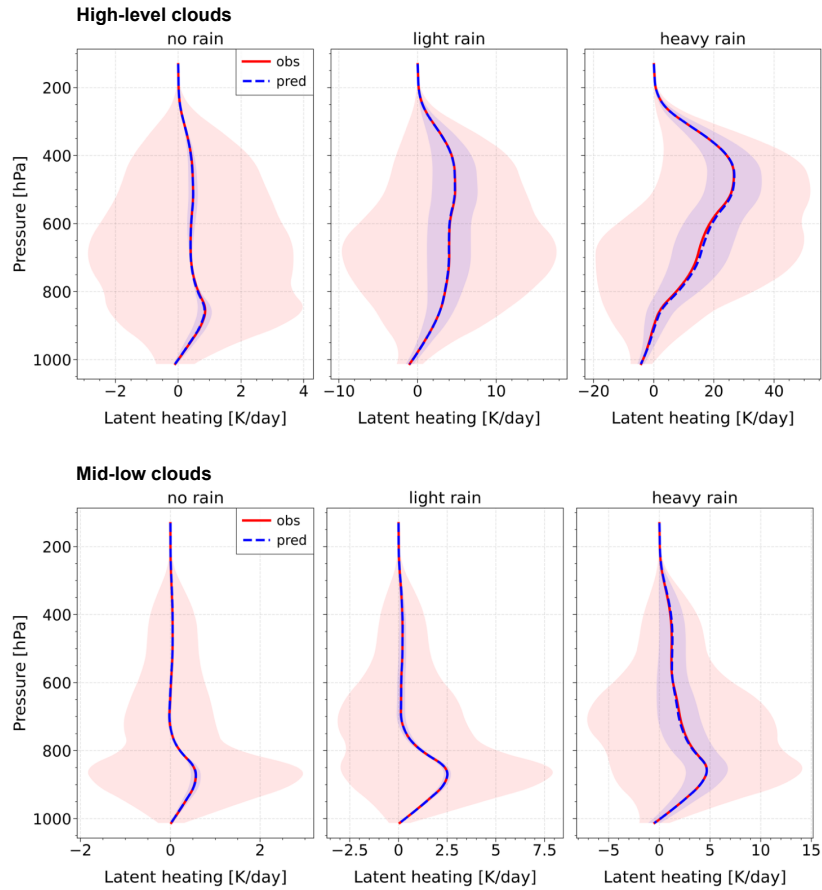


**Figure S6.** Average and range of predicted (dashed) and observed (solid) LH rates (2004–2013) of high-level clouds (top panels, same as the upper panels of Fig. 3, but with independent X-axis tick labels) and mid-low level clouds (bottom panels), for different rain rate intensities (no rain, light rain and heavy rain) over both ocean and land, within  $30^\circ\text{N}$ – $30^\circ\text{S}$ , with a spatial resolution of  $0.5^\circ$ . Models were trained on collocated AIRS–TRMM. Shaded areas indicate  $\pm 67.5^\circ$  of the standard deviation, which corresponds to quartiles.

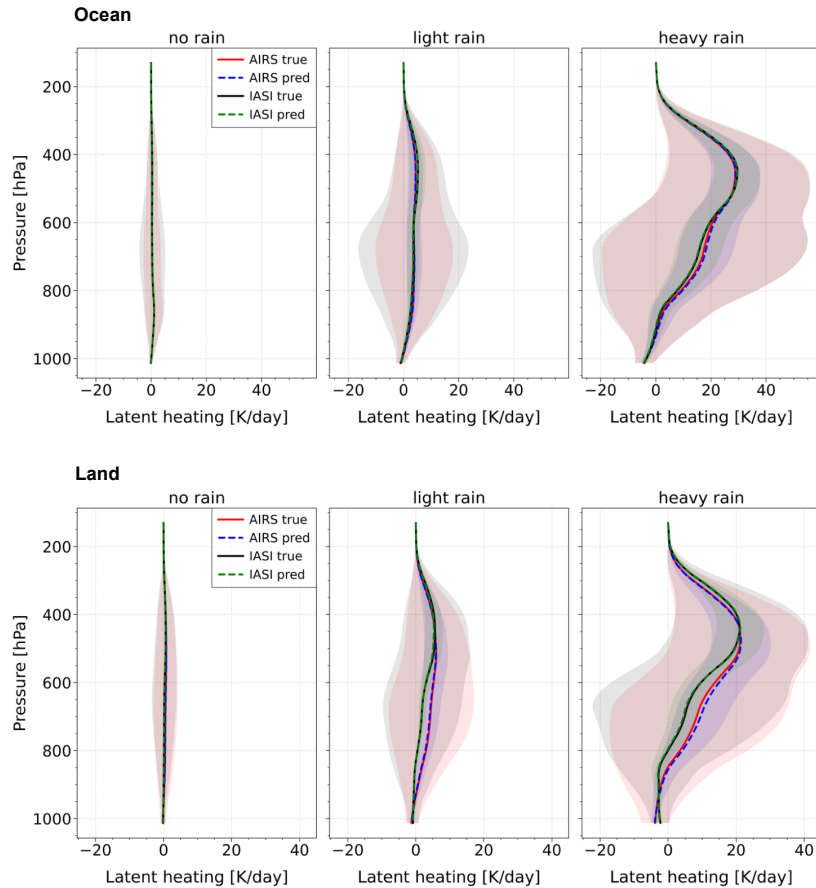


**Figure S7.** Average and range of predicted and observed LH rates for high-level clouds with different rain intensities (no rain, light rain and heavy rain), over ocean (top panels) and land (bottom panels), separately for AIRS and IASI, within  $30^\circ\text{N}$ – $30^\circ\text{S}$ , at a spatial resolution of  $0.5^\circ$ . Models were trained on collocated AIRS–TRMM and IASI–TRMM. Shaded areas indicate  $\pm 67.5^\circ$  of the standard deviation, which corresponds to quartiles.

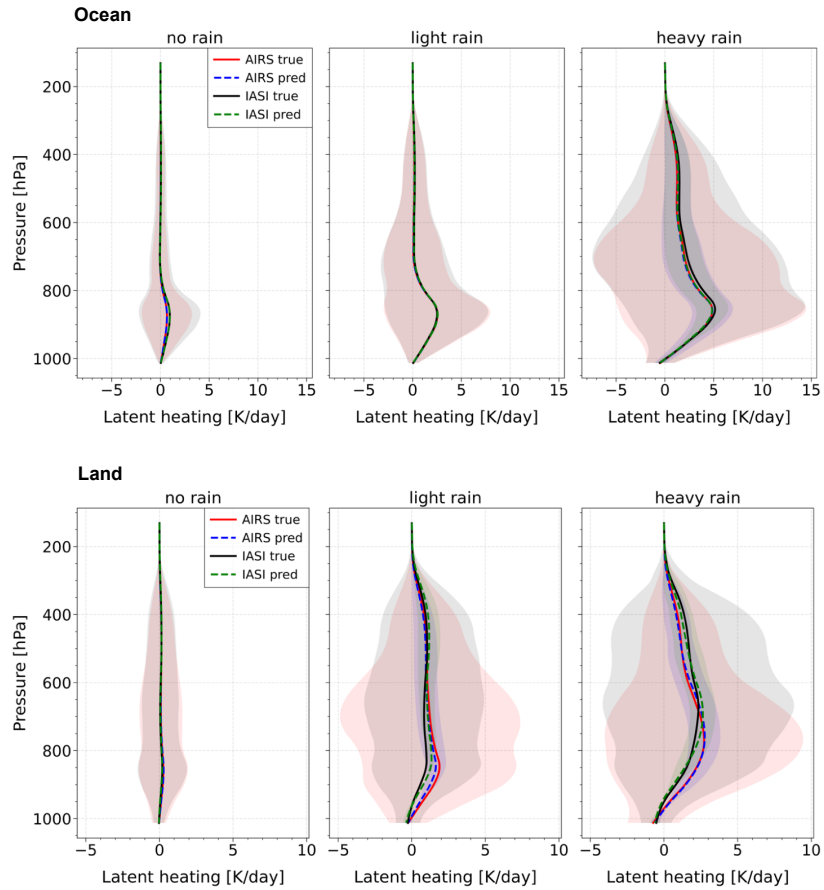


**Figure S8.** Average and range of between predicted and observed LH rates for mid-low level clouds with different rain intensities (no rain, light rain and heavy rain), over ocean (top panels) and land (bottom panels), separately for AIRS and IASI, within  $30^\circ\text{N}$ – $30^\circ\text{S}$ , at a spatial resolution of  $0.5^\circ$ . Models were trained on collocated AIRS–TRMM and IASI–TRMM. Shaded areas indicate  $\pm 67.5^\circ$  of the standard deviation, which corresponds to quartiles.

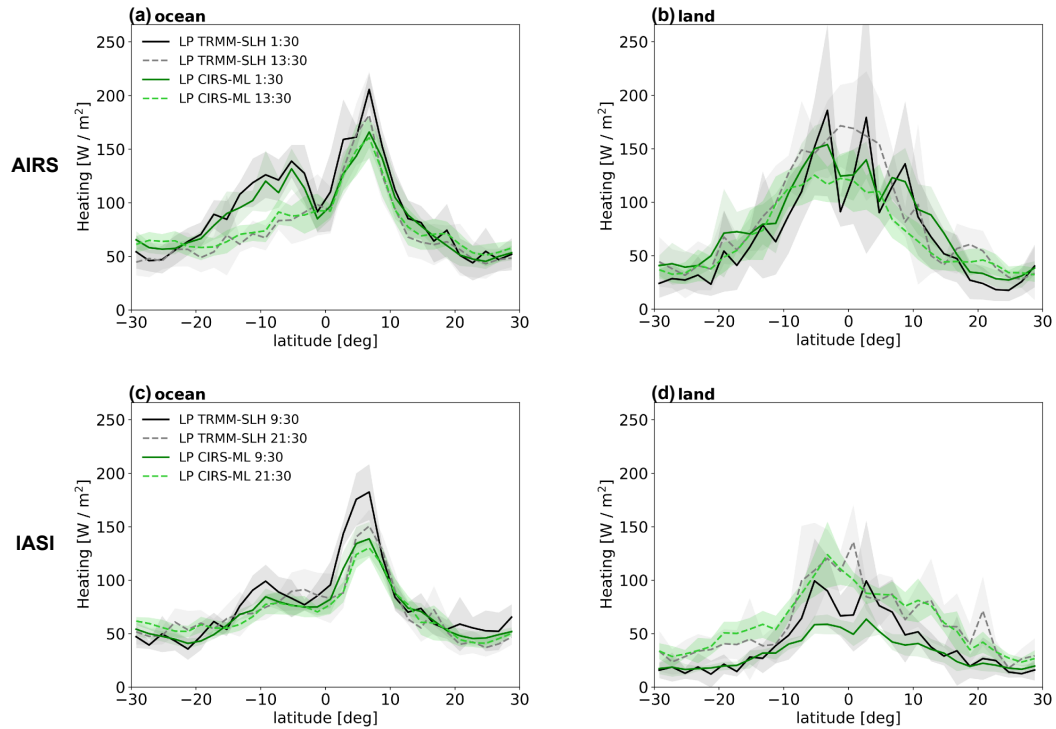


**Figure S9.** Zonal averages of vertically integrated LH (LP) of collocated data (a) at 1:30 AM and PM over ocean, (b) at 1:30 AM and PM over land, (c) at 9:30 AM and PM over ocean, (d) at 9:30 AM and PM over land. Black solid lines: TRMM LP for AM observations. Gray dashed line: TRMM LP for PM observations. Dark green solid line: LP from ML regression using AIRS or IASI as inputs for AM observations. Light green dashed line: LP from ML regression using AIRS or IASI as inputs for PM observations. Shaded areas correspond to inter-annual variabilities. The latitude intervals are  $2^\circ$ , and the time period is 2008-2013.

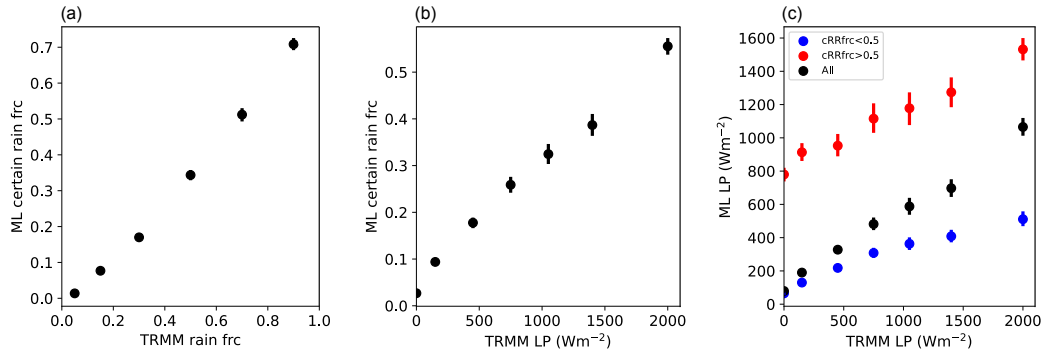


**Figure S10.** Average relationships for high-level clouds between (a) CIRS-ML certain rain fraction and TRMM rain fraction, (b) CIRS-ML certain rain fraction and TRMM-SLH LP and (c) CIRS-ML LP and TRMM-SLH LP for all and for cases with CIRS-ML certain rain fraction  $< 0.5$  and  $> 0.5$ . Statistics of collocated data over ocean  $30^{\circ}N-30^{\circ}S$ , over the time period from 2004–2013.

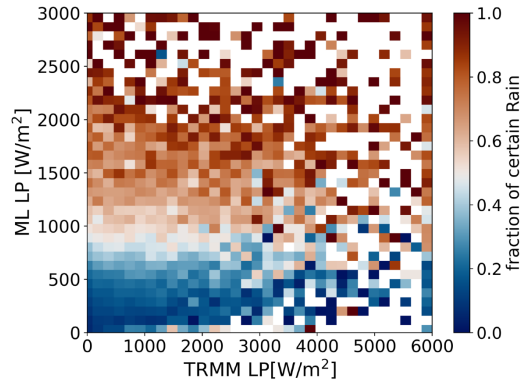


**Figure S11.** Averages of CIRS-ML certain rain fraction as function of TRMM-SLH LP and CIRS-ML LP of high-level clouds over the ocean, from collocated data for the period 2004–2013, spanning  $30^{\circ}N$  to  $30^{\circ}S$ , at a spatial resolution of  $0.5^{\circ}S$ . Each square corresponds to an interval of  $75 W m^{-2}$  in ML LP and  $150 W m^{-2}$  in TRMM-SLH LP.

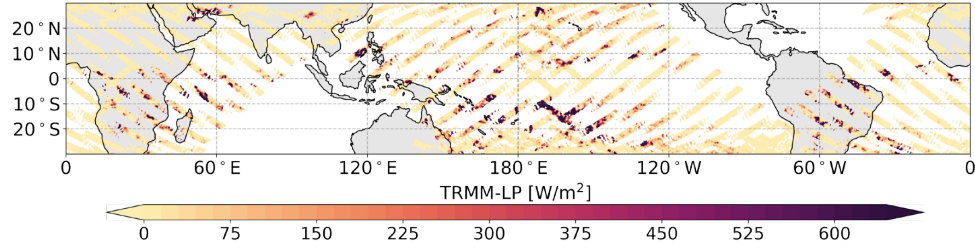


**Figure S12.** Maps of vertically integrated LH during La Niña (JAN 2008), within 30°N–30°S, at a spatial resolution of 0.5°. Data from TRMM-SLH, at 1h30 AM/PM (AIRS).

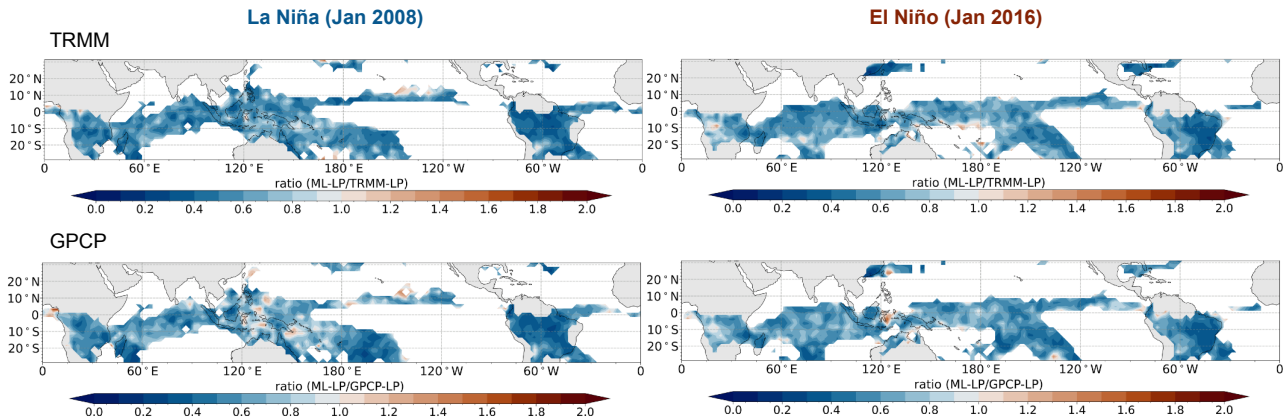


**Figure S13.** Ratio between the vertically integrated latent heating (LP) from CIRS–ML (at 1:30 LT) and the LP estimated from daily precipitation data from TRMM (upper panels) and GPCP (lower panels). The ratios (CIRS–ML LP / TRMM LP or GPCP LP) are shown for La Niña (JAN 2008) and El Niño (JAN 2016), over the region 30°N–30°S, at a spatial resolution of 2.5° × 2.5°. Since very small TRMM LP values could lead to unrealistic ratios, we apply a threshold of 50 W m<sup>-2</sup> to filter out these cases.

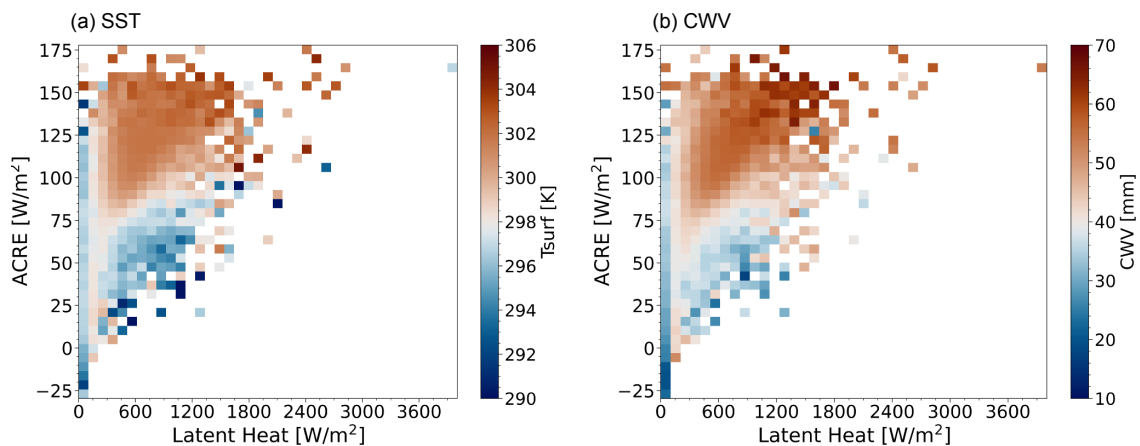


**Figure S14.** Averages of (a) SST and (b) CWV as function of LP and ACRE released by precipitating UT clouds over the ocean, for the period 2004–2013, spanning 30°N to 30°S, at a spatial resolution of 5°. LP and ACRE are from CIRS–ML, while SST and CWV are from ERA-Interim at 1:30 AM/PM local time. Each square corresponds to an interval of 75 W m<sup>-2</sup> in ML LP and 5.25 W m<sup>-2</sup> in ACRE.

**Table S1.** Validation MAE (K day<sup>-1</sup>) for the prediction of LH rates using models over different rain intensity classes.

Scene	Ocean / Land	No Rain	Light Rain	Heavy Rain
<b>AIRS</b>				
high-level clouds	ocean	0.024	0.146	0.552
	land	0.029	0.150	0.427
mid-low clouds	ocean	0.008	0.032	0.085
	land	0.008	0.042	0.058
<b>IASI</b>				
high-level clouds	ocean	0.027	0.158	0.541
	land	0.022	0.138	0.387
mid-low clouds	ocean	0.012	0.033	0.089
	land	0.007	0.043	0.065